

# Extraction of the neutron charge radius from a precision calculation of the deuteron structure radius

A. A. Filin,<sup>1</sup> V. Baru,<sup>2,3,4</sup> E. Epelbaum,<sup>1</sup> H. Krebs,<sup>1</sup> D. Möller,<sup>1</sup> and P. Reinert<sup>1</sup>

<sup>1</sup>*Ruhr-Universität Bochum, Fakultät für Physik und Astronomie,  
Institut für Theoretische Physik II, D-44780 Bochum, Germany*

<sup>2</sup>*Helmholtz-Institut für Strahlen- und Kernphysik and Bethe Center for Theoretical Physics, Universität Bonn, D-53115 Bonn, Germany*

<sup>3</sup>*Institute for Theoretical and Experimental Physics, B. Chermushkinskaya 25, 117218 Moscow, Russia*

<sup>4</sup>*P.N. Lebedev Physical Institute of the Russian Academy of Sciences, 119991, Leninskiy Prospect 53, Moscow, Russia*

We present a high-accuracy calculation of the deuteron structure radius in chiral effective field theory. Our analysis employs the state-of-the-art semilocal two-nucleon potentials and takes into account two-body contributions to the charge density operators up to fifth order in the chiral expansion. The strength of the fifth-order short-range two-body contribution to the charge density operator is adjusted to the experimental data on the deuteron charge form factor. A detailed error analysis is performed by propagating the statistical uncertainties of the low-energy constants entering the two-nucleon potentials and by estimating errors from the truncation of the chiral expansion as well as from uncertainties in the nucleon form factors. Using the predicted value for the deuteron structure radius together with the very accurate atomic data for the difference of the deuteron and proton charge radii we, for the first time, extract the charge radius of the neutron from light nuclei. The extracted value reads  $r_n^2 = -0.106_{-0.005}^{+0.007} \text{fm}^2$  and its magnitude is about  $1.7\sigma$  smaller than the current value given by the PDG. In addition, given the high-accuracy of the calculated deuteron charge form factor and its careful and systematic error analysis, our results open the way for an accurate determination of the nucleon form factors from elastic electron-deuteron scattering data measured at MAMI and other experimental facilities.

PACS numbers: 14.20.Dh, 13.40.Gp, 13.75.Cs, 12.39.Fe

The tremendous progress in atomic spectroscopy achieved in the last decade led to a series of high-precision measurements of the energy-level shifts in light atomic systems which are important for understanding the structure of light nuclei and their charge distributions. In particular, a series of extremely precise measurements of the hydrogen-deuterium 1S-2S isotope shift accompanied with an accurate theoretical QED analysis (see Ref. [1] for the latest update up through  $O(\alpha^2)$ ) resulted in the extraction of the deuteron-proton mean-square charge radii difference [2]

$$r_d^2 - r_p^2 = 3.82007(65) \text{fm}^2. \quad (1)$$

Due to its very high accuracy, this difference provides a tight link between  $r_d$  and  $r_p$  and thus is important in connection with the light nuclear charge radius puzzle. For many years, the values for  $r_p$  extracted from electron and muon experiments showed more than a  $5\sigma$  discrepancy [3]. The very recent atomic hydrogen measurements [4, 5], however, claim consistency with the analogous muonic hydrogen experiments. The recommended value for the proton root-mean-square charge radius has been changed to  $r_p = 0.8414(19) \text{fm}$  in the latest CODATA-2018 update [6], and the deuteron charge radius was updated accordingly, by virtue of the difference in Eq. (1). The updated CODATA deuteron charge radius is only  $1.9\sigma$  larger than the spectroscopic measurement on the muonic deuterium [7] but still  $2.9\sigma$  smaller than the  $r_d$  value from electronic deuterium spectroscopy [8].

From the nuclear physics perspective, the charge radius of the deuteron provides access to the deuteron internal structure through its structure radius, which is obtained from  $r_d^2$  by subtracting the contributions from the individual nucleons and the

relativistic (Darwin-Foldy) correction,

$$r_{\text{str}}^2 = r_d^2 - r_p^2 - r_n^2 - \frac{3}{4m_p^2}, \quad (2)$$

where  $m_p$  is the proton mass and  $r_n^2$  is the neutron mean square charge radius. Traditionally, this relation is used to determine  $r_{\text{str}}^2$  assuming that  $r_d^2 - r_p^2$  and  $r_n^2$  are known. The current value for the neutron charge radius quoted by the PDG is based on measurements of the neutron-electron scattering length in four different experiments carried out in 1973–1997 on  $^{208}\text{Pb}$ ,  $^{209}\text{Bi}$  and other heavy targets. The world average gives  $r_n^2 = -0.1161(22) \text{fm}^2$ , where the estimated error was increased by a scaling factor of 1.3 [9]. Nevertheless, the spread in the results on Pb and Bi is significantly larger than even the increased uncertainty quoted by the PDG, which suggests that the error for the neutron mean-square charge radius might be underestimated [10].

With the recent advances in chiral effective field theory ( $\chi$ EFT), theoretical analyses of low-energy few-nucleon reactions and nuclear structure enter the precision era [11–13]. In this letter we demonstrate that by employing the nuclear forces and currents derived up through fifth order in  $\chi$ EFT, a very accurate determination of  $r_{\text{str}}$  is becoming possible from the analysis of the deuteron charge form factor (FF). Equipped with this result and using the information from the hydrogen-deuterium isotope shift measurements given in Eq. (1), we use the relation (2) to extract, for the first time, the neutron mean square charge radius from the lightest atoms.

The electromagnetic FFs of the deuteron certainly belong to the most extensively studied observables in nuclear physics, see Ref. [14–16] for review articles. A large variety of theoretical approaches ranging from non-relativistic quantum me-

chanics to covariant models have been applied to this problem since the sixties of the last century, see Ref. [17] for an overview. The electromagnetic structure of the deuteron has also been investigated in the framework of pionless [18] and  $\chi$ EFT [19–25]. It is therefore crucial to emphasize the essential new aspects of the current investigation:

- For the first time the calculation of the deuteron charge FF is pushed to fifth order ( $N^4$ LO) in  $\chi$ EFT. This is achieved by (i) using the currently most accurate and precise  $\chi$ EFT two-nucleon (2N) potentials from Ref. [26] and (ii) taking into account the short-ranged contribution to the two-body charge density operator at  $N^4$ LO.
- The two-body charge density is regularized consistently with the 2N potential using the improved approach of Ref. [26], which maintains the long-range interactions. The residual cutoff dependence of our results is verified to be well within the truncation uncertainty.
- We employ the most up-to-date parametrizations of the nucleon FFs from the global analysis of experimental data [27, 28]. To estimate the corresponding systematic uncertainty, we also use the results from the dispersive analyses of Refs. [29–31], which incorporate constraints from unitarity and analyticity and predict the small proton radius consistent with the CODATA-2018 recommended value [6].
- A thorough analysis of various types of uncertainty in the calculated deuteron FFs and the structure radius is performed.

*Framework.* In the Breit frame, the deuteron charge form factor is expressed in terms of the matrix elements of the electromagnetic current, convolved with the deuteron wave functions as

$$G_C(Q^2) = \frac{1}{3e} \frac{1}{2P_0} \sum_{\lambda} \langle P', \lambda | J_B^0 | P, \lambda \rangle, \quad (3)$$

$$\frac{1}{2P_0} \langle P', \lambda' | J_B^\mu | P, \lambda \rangle = \int \frac{d^3 l_1}{(2\pi)^3} \frac{d^3 l_2}{(2\pi)^3} \times \quad (4)$$

$$\psi_{\lambda'}^\dagger \left( \mathbf{l}_2 + \frac{\mathbf{k}}{4}, \mathbf{v}_B \right) J_B^\mu \psi_{\lambda} \left( \mathbf{l}_1 - \frac{\mathbf{k}}{4}, -\mathbf{v}_B \right),$$

where  $e$  is the magnitude of electron charge,  $J_B^\mu$  is the four-vector current calculated in the Breit frame,  $\psi_\lambda$  is the deuteron wave function with polarization  $\lambda$  and the deuteron in the final (initial) state moves with the velocity  $\mathbf{v}_B$  ( $-\mathbf{v}_B$ ) with  $\mathbf{v}_B = \mathbf{k}/(2\sqrt{\mathbf{k}^2/4 + m_d^2}) = \hat{\mathbf{k}}\sqrt{\eta/(1+\eta)}$  along the photon momentum. The relativistic corrections to the deuteron wave functions related to the motion of the initial and final deuterons are included along the line of Ref. [32]. Furthermore, denoting the photon momentum  $k = (0, \mathbf{k})$  (with  $Q^2 = -k^2 \geq 0$ ) and the deuteron mass  $m_d$ , the deuteron initial and final momenta read  $P = (P_0, -\mathbf{k}/2)$  and  $P' = (P_0, +\mathbf{k}/2)$ , respectively, with  $P_0 = m_d\sqrt{1+\eta}$  and  $\eta = Q^2/(2m_d)^2$ .

The deuteron charge radius is defined as follows:

$$r_d^2 = (-6) \left. \frac{\partial G_C(Q^2)}{\partial Q^2} \right|_{Q^2=0}. \quad (5)$$

The calculation of the deuteron FFs requires two important ingredients which need to be derived in a consistent manner, namely the nuclear wave functions and the electromagnetic currents. The employed deuteron wave functions are calculated from the state-of-the-art  $\chi$ EFT 2N potentials of Ref. [26] which are among the most precise interactions on the market. Among many appealing features of these interactions, we especially benefit from a simple regularization scheme for the pion exchange contributions which (i) maintains the long-range part of the interaction, (ii) is applied in momentum space and (iii) allows for a straightforward generalization to current operators and many-body forces at tree level.

The nuclear electromagnetic charge and current operators have been recently worked out to  $N^3$ LO in  $\chi$ EFT using the method of unitary transformation [33–35] by our group and employing time-ordered perturbation theory [36–38] by the JLab-Pisa group, see also Ref. [39] for an early study along this line. The derivation of the electromagnetic currents and nuclear forces is carried out using the Weinberg power counting based on the expansion parameter  $Q = p/\Lambda_b$  with  $p \sim M_\pi$  being a characteristic soft momentum scale (with  $M_\pi$  denoting the pion mass) and  $\Lambda_b$  referring to the breakdown scale of the chiral expansion. This implies that the contributions to the charge operators relevant for our study appear at orders  $Q^{-3}$  (LO),  $Q^{-1}$  (NLO),  $Q^0$  ( $N^2$ LO),  $Q^1$  ( $N^3$ LO) and  $Q^2$  ( $N^4$ LO). To the order we are working, the single-nucleon contribution to the charge density operator in the kinematics  $N(p) + \gamma(k) \rightarrow N(p')$  takes a well-known form (see, e.g., Ref. [35] and references therein)

$$\rho_{1N} = e \left( 1 - \frac{\mathbf{k}^2}{8m_N^2} \right) G_E(\mathbf{k}^2) + ie \frac{G_{ME}}{4m_N^2} (\boldsymbol{\sigma} \cdot \mathbf{k} \times \mathbf{k}_1), \quad (6)$$

where  $\mathbf{k}_1 = (\mathbf{p} + \mathbf{p}')/2$ ,  $G_E(\mathbf{k}^2)$  and  $G_M(\mathbf{k}^2)$  are the electric and magnetic form factors of the nucleon,  $G_{ME} := 2G_M(\mathbf{k}^2) - G_E(\mathbf{k}^2)$ , and  $m_N$  denotes the nucleon mass. The term  $eG_E$  on the rhs of Eq. (6) emerges at LO, while all other terms start to contribute at  $N^3$ LO. Contributions to the two-body charge density first appear at  $N^3$ LO from one- and two-pion exchange diagrams, see Ref. [34] for explicit expressions. Most of them are of the isovector type and, therefore, do not contribute to the deuteron FFs. The only  $N^3$ LO operator relevant for our study, to be denoted as  $\rho_{2N}^{1\pi}$ , is a relativistic correction to the one-pion exchange. It is proportional to unobservable phases  $\bar{\beta}_8$  and  $\bar{\beta}_9$  which parameterize the unitary ambiguity of the long-range nuclear forces and currents at  $N^3$ LO. In contrast to nuclear potentials, observable quantities such as e.g. the form factors must, of course, be independent of the choice of  $\bar{\beta}_8$ ,  $\bar{\beta}_9$  and other off-shell parameters. This can only be achieved by using *off-shell consistent* expressions for the nuclear forces and currents. Specifically, to preserve consistency with semilocal 2N potentials

of Ref. [26], the one-pion exchange charge density has to be evaluated using the so-called minimal nonlocality choice with  $\bar{\beta}_8 = 1/4$  and  $\bar{\beta}_9 = -1/4$ . Although the pionic contributions to the isoscalar charge density at  $N^4$ LO have not been worked out yet, the complete expression for the contact operators at  $N^4$ LO reads [42] (the contact term relevant for the quadrupole moment of the deuteron was first derived in Ref. [18])

$$\rho_{2N}^{\text{cont}} = 2eG_E^S(\mathbf{k}^2) (A\mathbf{k}^2 + B\mathbf{k}^2(\boldsymbol{\sigma}_1 \cdot \boldsymbol{\sigma}_2) + C\mathbf{k} \cdot \boldsymbol{\sigma}_1 \mathbf{k} \cdot \boldsymbol{\sigma}_2),$$

where three low-energy constants (LECs)  $A, B$  and  $C$  contribute to the deuteron charge FF in *one* linear combination only, see supplementary material for details. The isoscalar electric nucleon form factor,  $G_E^S(\mathbf{k}^2)$ , is included in the two-body operators to account for a non-pointlike character of the  $NN\gamma$  vertex. The chiral expansion of the electromagnetic FFs of the nucleon is well known to converge slowly as they turn out to be dominated by the contributions of vector mesons [40, 41], which are not included as explicit degrees of freedom in  $\chi$ EFT. Therefore, to minimize the impact of the slow convergence of the chiral expansion of the nucleon FFs on 2N observables, we employ up-to-date parameterizations of the nucleon FFs from Ref. [28] as well as from several dispersive analyses of Refs. [29–31].

The 2N charge density operators  $\rho_{2N}^{1\pi}$  and  $\rho_{2N}^{\text{cont}}$  must be regularized consistently with the employed 2N potentials. In order to avoid short-range artifacts which could call into question reliability of the calculated observables, the 2N charge density operators have to be derived using the same regulator as employed in the 2N potentials. The regularization of the operators with the single pion propagator is worked out in Ref. [26] and can be effectively written as a substitution:

$$\frac{1}{\mathbf{p}^2 + M_\pi^2} \rightarrow \frac{1}{\mathbf{p}^2 + M_\pi^2} \exp\left(-\frac{\mathbf{p}^2 + M_\pi^2}{\Lambda^2}\right), \quad (7)$$

where  $\Lambda$  is a fixed cutoff chosen consistently with the employed 2N potential in the range of 400–550 MeV. The prescription for regularizing the squared pion propagator consistent with the approach used in [26] can be obtained from Eq. (7) by taking a derivative with respect to  $M_\pi^2$ . To maintain consistency between  $\rho_{2N}^{\text{cont}}$  and the corresponding short-range terms in the 2N potential after regularization, we exploit the fact that both can be generated from the same unitary transformation acting on the single-nucleon charge density and the kinetic energy term, respectively [42].

*Results and discussions.* The calculated deuteron FF at  $N^4$ LO,  $G_C^{\text{th}}(Q)$ , involves one unknown parameter (a combination of the LECs from  $\rho_{2N}^{\text{cont}}$ ), which is extracted from a fit to the world data for the deuteron charge form factor  $G_C^{\text{exp}}(Q)$  from Refs. [43–45]. Here and in what follows, the  $N^4$ LO results are obtained using the  $N^4$ LO<sup>+</sup> 2N potentials.

The function  $\chi^2$  to be minimized in the fit is defined as follows

$$\chi^2 = \sum_i \frac{(G_C^{\text{th}}(Q_i) - G_C^{\text{exp}}(Q_i))^2}{\Delta G_C(Q_i)^2}, \quad (8)$$

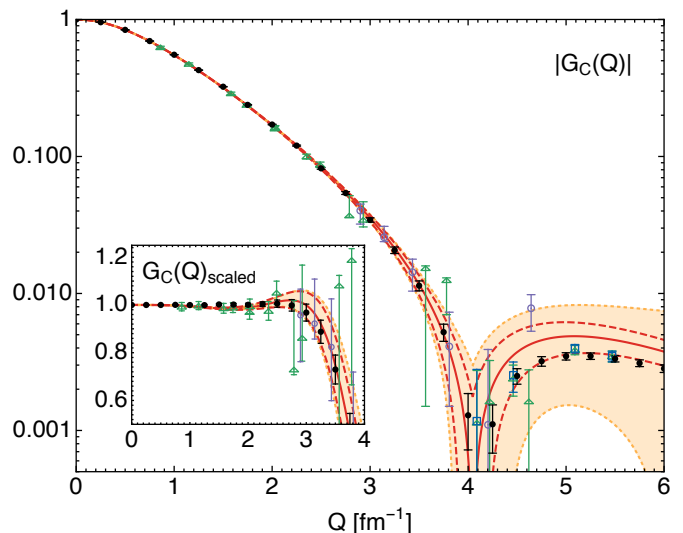


FIG. 1. (Color online) Deuteron charge FF from the best fit to data up to  $Q = 4 \text{ fm}^{-1}$  evaluated for the cutoff  $\Lambda = 500 \text{ MeV}$  (solid red lines). Band between dashed (red) lines corresponds to a  $1\sigma$  error in the determination of the short-range contribution to the charge density operator at  $N^4$ LO. Light-shaded (orange dotted) band corresponds to the estimated error (68% DoB) from truncation of the chiral expansion at  $N^4$ LO. Open violet circles, green triangles and blue squares are experimental data from Refs. [43], [44] and [45], respectively. Black solid circles correspond to the parameterization of the deuteron FFs from Ref. [16, 46] which is not used in the fit and shown just for comparison. The rescaled charge FF of the deuteron,  $G_C(Q)_{\text{scaled}}$ , as defined in Ref. [16], is shown on a linear scale.

TABLE I. Deuteron structure radius squared predicted at  $N^4$ LO in  $\chi$ EFT (1st column) and the individual contributions to its uncertainty: from the truncation of the chiral expansion (2nd), the statistical error in the short-range charge density operator extracted from  $G_C(Q^2)$  (3rd), the errors from the statistical uncertainty in  $\pi$ N LECs from the Roy-Steiner analysis of Ref. [50, 51] propagated through the variation in the deuteron wave functions (4th), the errors from the statistical uncertainty in 2N LECs from the analysis of the 2N observables of Ref. [26] (5th), the error from the choice of the maximal energy in the fit (6th) as well as the total uncertainty evaluated using the sum of these numbers in quadrature (7th). All numbers are given in  $\text{fm}^2$ .

$r_{\text{str}}^2$	truncation	$\rho_{2N}^{\text{cont}}$	$\pi$ N LECs	2N LECs	$Q$ -range	total
3.8933	$\pm 0.0032$	$\pm 0.0037$	$\pm 0.0004$	$+0.0010$ $-0.0047$	$\pm 0.0017$	$+0.0053$ $-0.0070$

where following Refs. [48, 49] the uncertainty  $\Delta G_C(Q_i)$  besides the experimental errors also takes into account theoretical uncertainties from the truncation of the chiral expansion estimated using the Bayesian approach and from the nucleon form factors, as given in Refs. [27, 28], added in quadrature. Throughout this analysis, we employ the Bayesian model  $C_{0.5-10}^{650}$  specified in Ref. [47] and assume the characteristic momentum scale to be given by  $|\mathbf{k}|/2$  [22]. The results for the deuteron charge FF from the best fit to data up to  $Q = 4$

$\text{fm}^{-1}$ , evaluated for the cutoff  $\Lambda = 500$  MeV, are visualized in Fig. 1 together with the  $N^4\text{LO}$  truncation errors and statistical uncertainty of the strength of  $\rho_{2N}^{\text{cont}}$ . We have verified that the cutoff variation in the range of  $\Lambda = 400 \dots 550$  MeV yields results lying well within the truncation error band and that the fits of a similar quality can be obtained by employing the nucleon FFs from the dispersive analyses of Refs. [29–31], see Ref. [42] for a detailed discussion of various uncertainties. The fit to data allows us to accurately extract the unknown linear combination of LECs entering the charge density operator at  $N^4\text{LO}$  and thus to make a parameter-free prediction for the structure radius of the deuteron, which reads

$$r_{\text{str}} = 1.9731_{-0.0018}^{+0.0013} \text{ fm}, \quad (9)$$

with the individual contributions to the uncertainty given in Table I. To make this uncertainty estimate conservatively, the truncation error is actually included twice: (i) by performing the Bayesian analysis for  $r_{\text{str}}^2$  following the approach of Ref. [47] and (ii) through the statistical uncertainty in the short-range charge density extracted from the fit to  $G_C^{\text{exp}}(Q^2)$  using Eq. (8). Furthermore, we developed a phase-equivalent version of the  $2N$  potential using a different choice of the unobservable phases  $\bar{\beta}_8 = \bar{\beta}_9 = 1/2$  leading to  $\rho_{2N}^{1\pi} = 0$ . Repeating the analysis for this choice of  $\bar{\beta}_{8,9}$ , the value of  $r_{\text{str}}$  is found to agree with the one in Eq. (9) to all given figures. The structure radius is also robust with respect to data used in the fit: had we used the parameterization of data by Sick [16, 46] instead of experimental data, we would have arrived at essentially the same result.

Relying on our theoretical prediction for the structure radius, we are now in the position to predict the neutron charge radius from Eqs. (1) and (2), which gives

$$r_n^2 = -0.106_{-0.005}^{+0.007} \text{ fm}^2. \quad (10)$$

This value is  $1.7\sigma$  smaller than the one given by the PDG [9].

In summary, we presented a comprehensive analysis of the deuteron charge form factor up to fifth order in  $\chi\text{EFT}$ . The only unknown parameter enters the short-range  $2N$  contribution to the charge density operator and is determined from the best fit to the deuteron charge form factor. Equipped with this information, we make a parameter-free prediction for the structure radius of the deuteron and perform a thorough analysis of various kinds of uncertainty. The high-accuracy calculation of the structure radius, together with the high-precision measurement of the hydrogen-deuterium  $1S$ - $2S$  isotope shift [2], have allowed us to extract the neutron charge radius.

Although it is natural to expect that the two-pion exchange contributions to the charge density at  $N^4\text{LO}$ , which have not yet been worked out, are largely saturated by the short-range contributions included in this analysis, the complete  $\chi\text{EFT}$  calculation at this order would allow for an additional test of the estimated theoretical uncertainty.

The results for the deuteron charge FF presented here pave the way for an accurate determination of the isoscalar nucleon

FF by (re)analyzing the experimental data on elastic electron-deuteron scattering at MAMI (see e.g. Ref. [52] for the new measurement of the elastic  $ed$  scattering cross section at  $0.24 \text{ fm}^{-1} \leq Q \leq 2.7 \text{ fm}^{-1}$  at MAMI), Saclay [53] and other facilities.

**Acknowledgments.** We are grateful to U.-G. Meißner for a careful reading of the manuscript and valuable comments and to Z. Ye for providing us with the unpublished results for the nucleon form factors from Ref. [28]. We also thank H.-W. Hammer for providing us with the parameterization of the nucleon form factors from Ref. [29] and I. Sick for the parameterization of the deuteron form factors from Ref. [16]. We are grateful to M. Hoferichter and J. Ruiz de Elvira for the information on the central values and covariance matrix of the  $N^4\text{LO}$   $\pi N$  LECs from the Roy-Steiner analysis. This work was supported in part by DFG and NSFC through funds provided to the Sino-German CRC 110 ‘‘Symmetries and the Emergence of Structure in QCD’’ (NSFC Grant No. 11621131001, Grant No. TRR110), the BMBF (Grant No. 05P18PCFP1) and the Russian Science Foundation (Grant No. 18-12-00226).

- 
- [1] K. Pachucki, V. Patkóš and V. A. Yerokhin, Phys. Rev. A **97**, no. 6, 062511 (2018).
  - [2] U. D. Jentschura *et al.*, Phys. Rev. A **83**, 042505 (2011).
  - [3] R. Pohl, R. Gilman, G. A. Miller and K. Pachucki, Ann. Rev. Nucl. Part. Sci. **63**, 175 (2013).
  - [4] A. Beyer *et al.*, Science **358**, no. 6359, 79 (2017).
  - [5] N. Bezginov, T. Valdez, M. Horbatsch, A. Marsman, A. C. Vutha and E. A. Hessels, Science **365**, no. 6457, 1007 (2019).
  - [6] E. Tiesinga, P. J. Mohr, D. B. Newell, and B. N. Taylor (2019), ‘‘The 2018 CODATA Recommended Values of the Fundamental Physical Constants’’ (Web Version 8.0). Database developed by J. Baker, M. Douma, and S. Kotochigova. Available at <http://physics.nist.gov/constants>, National Institute of Standards and Technology, Gaithersburg, MD 20899.
  - [7] R. Pohl *et al.* [CREMA Collaboration], Science **353**, no. 6300, 669 (2016).
  - [8] R. Pohl *et al.*, Metrologia **54**, no. 2, L1 (2017).
  - [9] M. Tanabashi *et al.* [Particle Data Group], Phys. Rev. D **98**, no. 3, 030001 (2018).
  - [10] L. V. Mitsyna, V. G. Nikolenko, S. S. Parzhitski, A. B. Popov and G. S. Samosvat, Nucl. Phys. A **819**, 1 (2009).
  - [11] E. Epelbaum, H.-W. Hammer and U.-G. Meißner, Rev. Mod. Phys. **81**, 1773 (2009).
  - [12] R. Machleidt and D. R. Entem, Phys. Rept. **503**, 1 (2011).
  - [13] E. Epelbaum, arXiv:1908.09349 [nucl-th].
  - [14] M. Garcon and J. W. Van Orden, Adv. Nucl. Phys. **26**, 293 (2001).
  - [15] R. A. Gilman and F. Gross, J. Phys. G **28**, R37 (2002).
  - [16] L. E. Marcucci *et al.*, J. Phys. G **43**, 023002 (2016).
  - [17] D. R. Phillips, Nucl. Phys. A **737**, 52 (2004).
  - [18] J. W. Chen, G. Rupak and M. J. Savage, Nucl. Phys. A **653**, 386 (1999).
  - [19] D. R. Phillips and T. D. Cohen, Nucl. Phys. A **668**, 45 (2000).
  - [20] M. Walzl and U.-G. Meißner, Phys. Lett. B **513**, 37 (2001).

- [21] D. R. Phillips, Phys. Lett. B **567**, 12 (2003).
- [22] D. R. Phillips, J. Phys. G **34**, 365 (2007).
- [23] M. P. Valderrama, A. Nogga, E. Ruiz Arriola and D. R. Phillips, Eur. Phys. J. A **36**, 315 (2008).
- [24] M. Piarulli, L. Girlanda, L. E. Marcucci, S. Pastore, R. Schiavilla and M. Viviani, Phys. Rev. C **87**, no. 1, 014006 (2013).
- [25] E. Epelbaum, A. M. Gasparyan, J. Gegelia and M. R. Schindler, Eur. Phys. J. A **50**, 51 (2014).
- [26] P. Reinert, H. Krebs and E. Epelbaum, Eur. Phys. J. A **54**, no. 5, 86 (2018).
- [27] Z. Ye, J. Arrington, R. J. Hill and G. Lee, Phys. Lett. B **777**, 8 (2018).
- [28] Z. Ye, private communication; An analysis of the nucleon EM FFs completely analogous to that in Ref. [27] is carried out using the input for the proton charge radius from CODATA-2018.
- [29] M. A. Belushkin, H.-W. Hammer and U.-G. Meißner, Phys. Rev. C **75**, 035202 (2007).
- [30] I. T. Lorenz, H.-W. Hammer and U.-G. Meißner, Eur. Phys. J. A **48**, 151 (2012).
- [31] I. T. Lorenz, U.-G. Meißner, H.-W. Hammer and Y.-B. Dong, Phys. Rev. D **91**, no. 1, 014023 (2015).
- [32] R. Schiavilla and V. R. Pandharipande, Phys. Rev. C **65**, 064009 (2002).
- [33] S. Kölling, E. Epelbaum, H. Krebs and U.-G. Meißner, Phys. Rev. C **80**, 045502 (2009).
- [34] S. Kölling, E. Epelbaum, H. Krebs and U.-G. Meißner, Phys. Rev. C **84**, 054008 (2011).
- [35] H. Krebs, E. Epelbaum and U.-G. Meißner, Few Body Syst. **60**, no. 2, 31 (2019).
- [36] S. Pastore, R. Schiavilla and J. L. Goity, Phys. Rev. C **78**, 064002 (2008).
- [37] S. Pastore, L. Girlanda, R. Schiavilla, M. Viviani and R. B. Wiringa, Phys. Rev. C **80**, 034004 (2009).
- [38] S. Pastore, L. Girlanda, R. Schiavilla and M. Viviani, Phys. Rev. C **84**, 024001 (2011).
- [39] T.-S. Park, D.-P. Min and M. Rho, Nucl. Phys. A **596**, 515 (1996).
- [40] B. Kubis and U.-G. Meißner, Nucl. Phys. A **679**, 698 (2001).
- [41] M. R. Schindler, J. Gegelia and S. Scherer, Eur. Phys. J. A **26**, 1 (2005).
- [42] A. A. Filin, D. Möller, V. Baru, E. Epelbaum, H. Krebs and P. Reinert, in preparation.
- [43] D. M. Nikolenko *et al.*, Phys. Rev. Lett. **90**, 072501 (2003).
- [44] D. Abbott *et al.* [JLAB t20 Collaboration], Eur. Phys. J. A **7**, 421 (2000).
- [45] D. Abbott *et al.* [JLAB t(20) Collaboration], Phys. Rev. Lett. **84**, 5053 (2000).
- [46] I. Sick, private communication.
- [47] E. Epelbaum *et al.*, arXiv:1907.03608 [nucl-th].
- [48] B. D. Carlsson *et al.*, Phys. Rev. X **6**, 011019 (2016).
- [49] S. Wesolowski, R. J. Furnstahl, J. A. Melendez and D. R. Phillips, J. Phys. G **46**, 045102 (2019).
- [50] M. Hoferichter, J. Ruiz de Elvira, B. Kubis and U.-G. Meißner, Phys. Rept. **625**, 1 (2016).
- [51] M. Hoferichter, J. Ruiz de Elvira, B. Kubis and U.-G. Meißner, Phys. Rev. Lett. **115**, no. 19, 192301 (2015).
- [52] B. S. Schlimme *et al.*, EPJ Web Conf. **113**, 04017 (2016).
- [53] S. Platchkov *et al.*, Nucl. Phys. A **510**, 740 (1990).